Prospects for Supersymmetry discovery with the ATLAS detector at the LHC running at 10 TeV centre-of-mass energy

Ilya Feige,
Institute of Particle Physics

August 20, 2009

Abstract

We study the discovery potential of supersymmetry with the ATLAS detector at the LHC. We assume an LHC running scenario of 10 TeV centre-of-mass energy with an integrated luminosity of 200 pb^{-1} for the 2009-2010 run. The analysis we use is model independent, however we investigate only the mSUGRA SU4 supersymmetry phase-space point in this study.

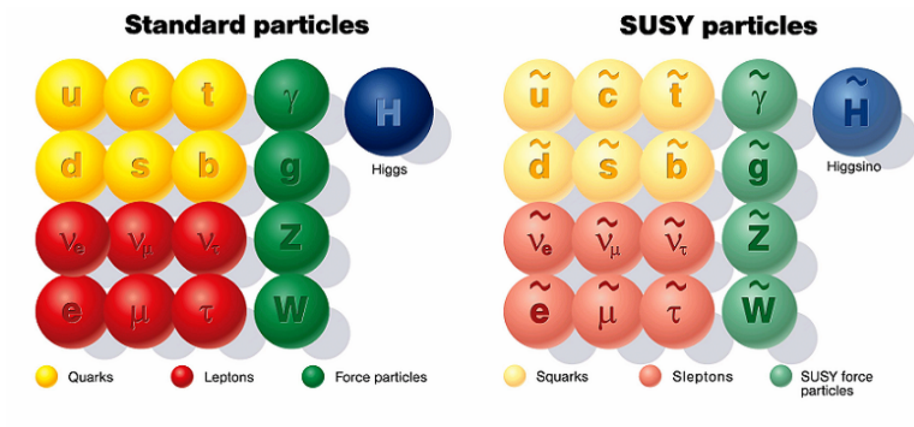

Figure 1: The Standard Model particles are shown on the left with their corresponding superpartners on the right.

1 Introduction

Supersymmetry

Supersymmetry (SUSY) is a proposed symmetry of nature that relates each elementary particle of a given spin to another of a spin differing by a half unit. That is, in a supersymmetric theory, for every boson there is a corresponding fermion and vice-versa. In order to incorporate supersymmetry into the Standard Model, we require the existence of a supersymmetric particle, coined a 'sparticle', for every Standard Model particle, this is shown in Figure 1.

There are many theoretical thorns in the Standard Model that supersymmetry may solve. The first attempt to incorporate supersymmetry into the Standard Model was done to solve the Hierarchy Problem. This is the problem of why the Higgs boson is so much lighter than the Planck mass. One would expect the Higgs mass to be on the order of the scale at which new physics appears – expected to be the Planck scale – due to quadratically diverging radiative corrections. In the Standard Model, keeping the Higgs mass light requires incredible fine-tuning in order to get cancellation of the diverging radiative corrections. This is avoided by having automatic cancellations between fermionic and bosonic Higgs interactions rendered possible by supersymmetry. This is shown in Figure 2, where the quadratic mass renormalisation due to the fermionic top quark loop is cancelled by the corresponding scalar stop squark loop diagram in the supersymmetric Standard Model.

Supersymmetry also makes other nice predictions, of which, the unification of the forces of Nature is possible. Since supersymmetry changes the extrapolation of the coupling constants of the forces, with supersymmetry we are able to get unification of these couplings at high energy, as shown in Figure 3.

Finally, supersymmetry proposes a natural dark matter candidate particle.

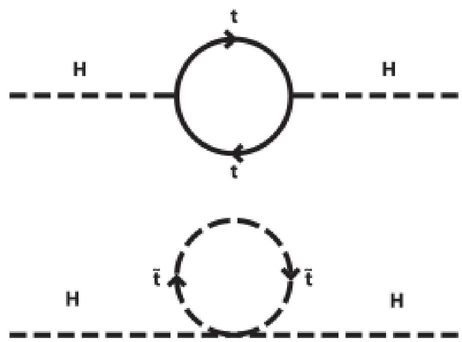

Figure 2: In the supersymmetric extension of the Standard Model the above two diagrams give cancelling contributions. Thus we get cancellation of the Higgs quadratic mass renormalisation between the fermionic top quark loop and the scalar stop squark loop diagram.

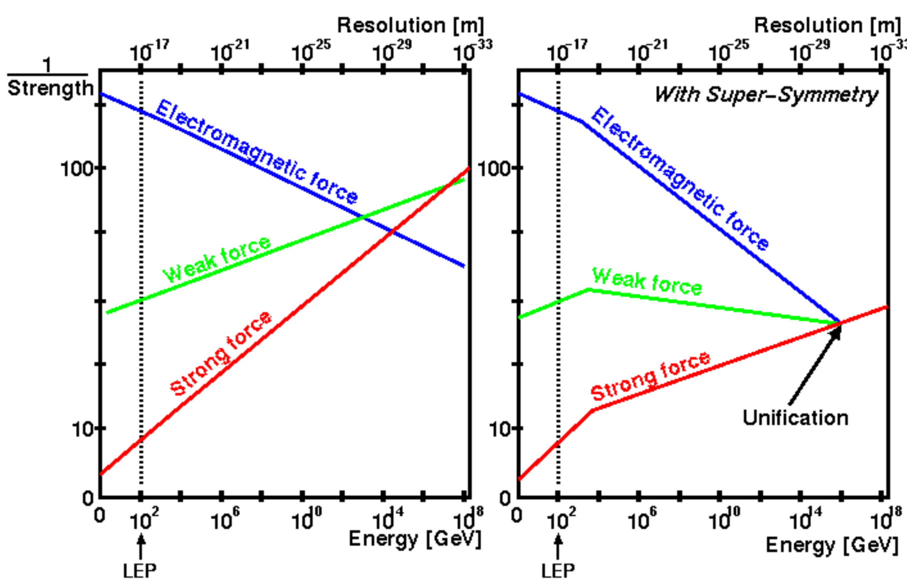

Figure 3: On the left, the extrapolation of the coupling constants for the Standard Model, and on the right that of the supersymmetric extension to the Standard Model.

In order to have conservation of baryonic and leptonic quantum numbers, a new multiplicative quantum number must be introduced called R-parity. R-parity is 1 for Standard Model particles and -1 for the supersymmetric partners. Models in which R-parity is violated can be formulated, but are usually not favoured due to proton stability among other reasons, so we will focus on R-parity conserving supersymmetric models. The consequences of R-parity conservation are that sparticles must be created in pairs, and that each will decay to the lightest supersymmetric particle (LSP) which must be stable. If the LSP were weakly interacting we would have a natural dark matter candidate[1][2].

Supersymmetry and the ATLAS detector

Assuming that the stable LSPs are weakly interacting, we expect them to pass undetected through the ATLAS detector. Thus we expect a characteristic feature of SUSY events: an imbalance in the transverse energy measured in the detector,[1] which we will denote $\not{E}_T$ and refer to as the missing transverse energy[2]. We also generally expect many jets and leptons with high transverse momentum, denoted P_T. A typical SUSY decay, producing large $\not{E}_T$ and a high multiplicity of high P_T jets and leptons, is shown in Figure 4. Since there are many supersymmetry models, with many parameters, we must make our searches as model independent as possible. Thus, in searching for generic R-parity conserving SUSY signatures, we simply look for an excess of events in various search channels. In this study we used channels with (≥ 2, ≥ 3, ≥ 4) jets, (0 - 2) leptons and having high $\not{E}_T$.[2] We assume an LHC centre-of-mass energy of 10 TeV and an integrated luminosity of 200 pb^{-1}. Though the analysis that we employed was model independent, we used a SUSY Monte Carlo dataset from the SU4 point in the mSUGRA parameter space. mSUGRA (minimal super gravity) is a class of models in which SUSY breaking is mediated by the gravitational interaction[2]. The important aspect, at this level, of the mSUGRA models is that they have high predictive power since they require only four input parameters and a sign.

In this report we systematically reproduced the results found in [3].

2 Analysis

Data

All of the samples used in this analysis were from Monte Carlo simulations. A discussion of the Monte Carlo simulations can be found in both [3] and [4]. We analysed on the order of 10 TBs of data. Acquisition and first manipulation of this data was done on the Grid. Subsequent manipulation and analysis was done locally using the ROOT framework.

[1]The transverse plane is the plane perpendicular to the beam axis.
[2]In this report, leptons are understood as muons and electrons.

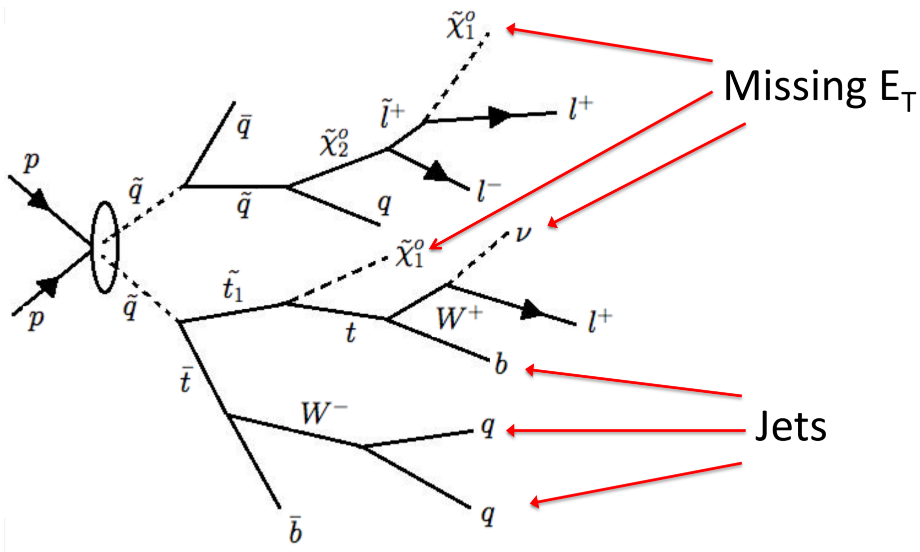

Figure 4: A typical SUSY cascade.

Object Identification

Separating events into the different search channels that we used requires an initial object identification that is common to all channels. This object identification defines particle candidates. We will need to used the detector's angular coordinates (ϕ, η), where ϕ is the angle in the transverse plane measured from the centre of the LHC ring, and $\eta = -\log \tan \theta/2$, where θ is the angle from the beam axis. We also define the geometric variable $\Delta R = \sqrt{\Delta\phi^2 + \Delta\eta^2}$. The object identification criteria are the following:

- Jets are reconstructed in a cone with an angular size of 0.4 in (ϕ, η), and are required to have a $P_T > 20$ GeV and $|\eta| < 2.5$ to ensure proper jet calibration. The $|\eta| < 2.5$ is the extent of the inner tracker.

- Electrons must pass the "medium" purity cuts[4], which include E_T dependent isolation criteria. They must also have $P_T > 10$ GeV and $|\eta| < 2.5$.

- Muons are reconstructed by matching the track reconstructed in the muon spectrometer with its corresponding inner detector track[4]. To ensure the muons selected are isolated, it is required that the total energy in the calorimeter within a cone of $\Delta R < 0.2$ is less than 10 GeV. We further require that the standard acceptance cuts of $P_T > 10$ GeV and $|\eta| < 2.5$ are passed.

We then impose an overlap removal policy for overlapping objects that pass the object identification criteria above. The overlap removal criteria are applied in the following order:

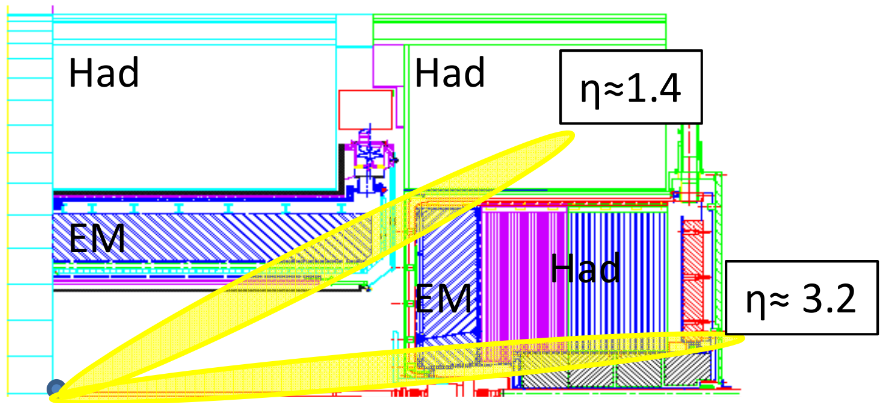

Figure 5: Barrel-endcap transition region of the electromagnetic calorimeter at $\eta \approx 1.4$.

1. If an electron and a jet are found within $\Delta R < 0.2$, discard the jet and keep the electron.
2. If a muon and a jet are found within $\Delta R < 0.4$, discard the muon and keep the jet.
3. If an electron and a jet are found within $0.2 \leq \Delta R < 0.4$, discard the electron and keep the jet.

In each case the above overlap rules discard an object that is expected to have come from the other. For instance, in the case of 2, it is supposed that the muon was from a decay particle within the jet, and not from the interaction being investigated[3].

Event Selection

The first event selection criteria is that no electrons are reconstructed in the barrel-endcap transition region of the electromagnetic calorimeter, $1.37 < |\eta| < 1.52$. There are cables running through this region, and thus we will not reconstruct objects in a well understood manner in early data. This region is shown in Figure 5. The following event variables will be used in the cuts defining the various search channels:

- **Effective Mass** (M_{eff}):

$$M_{eff} = \sum_{i=1}^{N_{jets}} {}^{jet}P_T^i + \sum_{i=1}^{N_{leps}} {}^{lep}P_T^i + \not{E}_T$$

  Where N_{jets} is the number of jets ($\in \{2,3,4\}$) and N_{lep} is the number of leptons ($\in \{0,1,2\}$) defining the search channel. Other high P_T jets or leptons are not included in the sum.

Number of jets	≥ 2 jets	≥ 3 jets	≥ 4 jets
Leading jet P_T (GeV)	>180	>100	>100
Jet P_T (GeV)	>50 (jet 2)	>40 (jet 2-3)	>40 (jet 2-4)
$\not{E}_T > \max(80\text{ GeV},\ f \cdot M_{eff})$	$f = 0.3$	$f = 0.25$	$f = 0.2$
$\Delta(jet_i,\ \not{E}_T)$	> 0.2 for the defining jets in the channel		
S_T	> 0.2		

Table 1: Cuts on the P_T of the leading jet, the P_T of the other jets, the $\not{E}_T$, the angle between each jet (of the 2, 3 or 4 jets) and the $\not{E}_T$ vector, and the transverse sphericity as a function of the minimum number of jets required.

- **Transverse Mass** (M_T) is defined only for the 1 lepton channel as:

  $$M_T = \sqrt{2\, P_T^{lep}\, \not{E}_T\, (1 - \cos\Delta\phi)}$$

  Where $\Delta\phi$ is the angle between the lepton and the missing energy in the plane perpendicular to the beam axis.

- **Transverse Sphericity** (S_T):

  $$S_T = \frac{2\,\lambda_2}{\lambda_1 + \lambda_2}$$

  Where λ_1 and λ_2 are the eigenvalues ($\lambda_1 > \lambda_2$) of the 2×2 sphericity tensor $S_{ij} = \sum_k p_{ki} p^{kj}$, where k runs over all selected jets and leptons.

Each channel must pass one column of cuts listed in Table 1, which defines the number of jets in that channel, and must satisfy one of the following:

- **Zero-lepton channels**: No leptons with $P_T > 20$ GeV.
- **One-lepton channels**: One lepton with $P_T > 20$ GeV and no others with $P_T > 10$ GeV, and $M_T > 100$ GeV.
- **Two-leptons channels**: Two leptons with $P_T > 10$ GeV and opposite charge.

This defines the nine non-mutually exclusive channels that will be used in our SUSY search. The cuts on the number of jets and their transverse momentum are chosen to be in accordance with the multijet trigger requirements (that is, they are harder cuts than the trigger makes at runtime) and to reject a sufficient amount of QCD jet background[3].

The S_T and $\Delta(jet_i,\ \not{E}_T)$ cuts

The motivation for the S_T and $\Delta(jet_i,\ \not{E}_T)$ cuts is that QCD light jet events are the hard scattering of quarks and are thus very "back-to-back", as shown in Figure 6 on the right. Therefore they have a small S_T (note that a perfectly

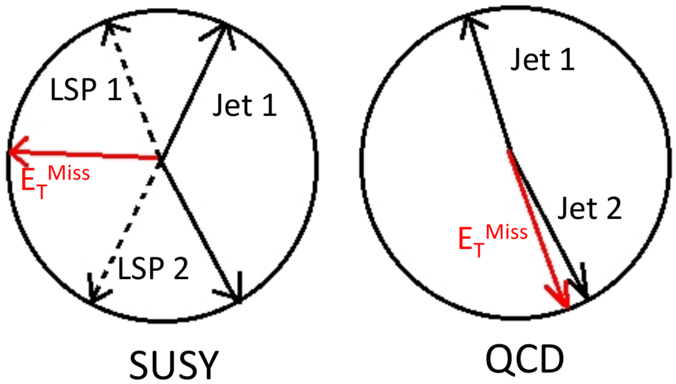

Figure 6: A simplified SUSY event on the left and QCD light jet event on the right.

"back-to-back" event has $S_T = 0$ and a perfectly spherical event has $S_T = 1$). By this same token, QCD light jet events have non-isolated $\not{E}_T$ (which corresponds to $\Delta(jet_1,\ \not{E}_T) \approx 0$ and $\Delta(jet_2,\ \not{E}_T) \approx \pi$) since they do not produce undetectable primary particles, so all of the $\not{E}_T$ comes from miscalibrated jets or neutrinos from particle decays within the jets. On the other hand, SUSY events often produce many leptons and jets and heavy-undetected particles, which leave large isolated $\not{E}_T$. Thus SUSY events are quite spherical and have large $\Delta(jet_i,\ \not{E}_T)$ for each jet, as shown in Figure 6 on the left. This makes these two cuts an effective method of removing the QCD background which has a very large cross section in the LHC running scenario under consideration.

3 Results

To perform the SUSY search in a model independent fashion, the effective mass distribution is used to find deviations between the Standard Model plus the signal and the expected Standard Model background. The significance of a discovery can then be optimised by varying the $M_{eff} > X$ GeV cut.

Plots of missing transverse energy and effective mass for the zero-lepton channel are shown in Figure 7 and Figure 8, respectively. The dominant background for the two-jet channel is that from the Z and W, whereas for the three and four-jet channels the dominant background is $t\bar{t}$ pair production. In all channels, however, the signal lies well above the background. It should be noted that the outlying bin – at around 3300 GeV – in each of the two lower plots in Figure 8 is from one QCD light jet event that passed the cuts for both the 3 and 4 jet channels with an event weight of ≈ 24.[3]

The one-lepton channel effective mass distribution is shown in Figure 9. We

[3] This event corresponds to run number 108365 and event number 107668, it has $.30 < S_T$ and $\min_i \left(\Delta(jet_i, \not{E}_T)\right) < .31$. The interested reader may want to do an event display of this anomalous event.

see that the primary background in all channels is that from $t\bar{t}$ pair production. We note that requiring a lepton effectively removes all of the QCD background. In these channels we see a much higher signal over background than in the zero-lepton channels but we have an order of magnitude fewer events. In most bins the signal plus background is an order of magnitude higher than the background. The reduced background is attributed to requiring a lepton, and the M_T cut. The M_T distribution for the one-lepton channels is shown in Figure 10, where these events have passed all but the $M_T > 100$ GeV cuts. There is a resonance in the $t\bar{t}$ and W backgrounds at 80 GeV – the W mass – after which both backgrounds fall off much more quickly than the SUSY signal, making for a powerful M_T cut.

The effective mass distribution for the two-lepton channels is shown in Figure 11. The major background in these channels is that from $t\bar{t}$ pair production.[4]

4 Discussion

From the plots in Figures 8-11, we see that in most channels the signal lies well above the background. What must be done to quantify this is to compute the significance of this difference. To do this would require an estimate of the errors on the various backgrounds. Common such estimates find these errors to be around 50%, including systematics[3][4]. However, these estimates are still rough, and require data-driven background measurements to improve them. With appropriate errors on the relevant quantities in this study, the discovery reach of our results could be computed. This analysis is done in [3] for the same LHC running scenario as we have used, and shows that a 5σ discovery can be made for a large-unexplored region of the SUSY phase space. We have not computed the significance nor made an attempt at a discovery reach plot due to lack of time. However the framework is built to reproduce these results, and the former would be a natural extension to this study.

5 Conclusions

The background composition and SUSY SU4 signal have been investigated for channels with 0, 1 and 2 opposite signed leptons and ≥ 2, ≥ 3 and ≥ 4 jets for an LHC running scenario of 10 TeV centre-of-mass energy and an integrated luminosity of 200 pb^{-1}. The results of this analysis show that in many channels the signal lies an order of magnitude above the background, but to quantify this in terms of discovery potential, we would need to compute the significance of the measurements presented in this study. This is the natural following step, and given that the framework has been laid it would be a smooth step to make. We hope that this report will incite a reader to follow up on the work that has been presented here.

[4] The official ATLAS results for this study can be found in [3]

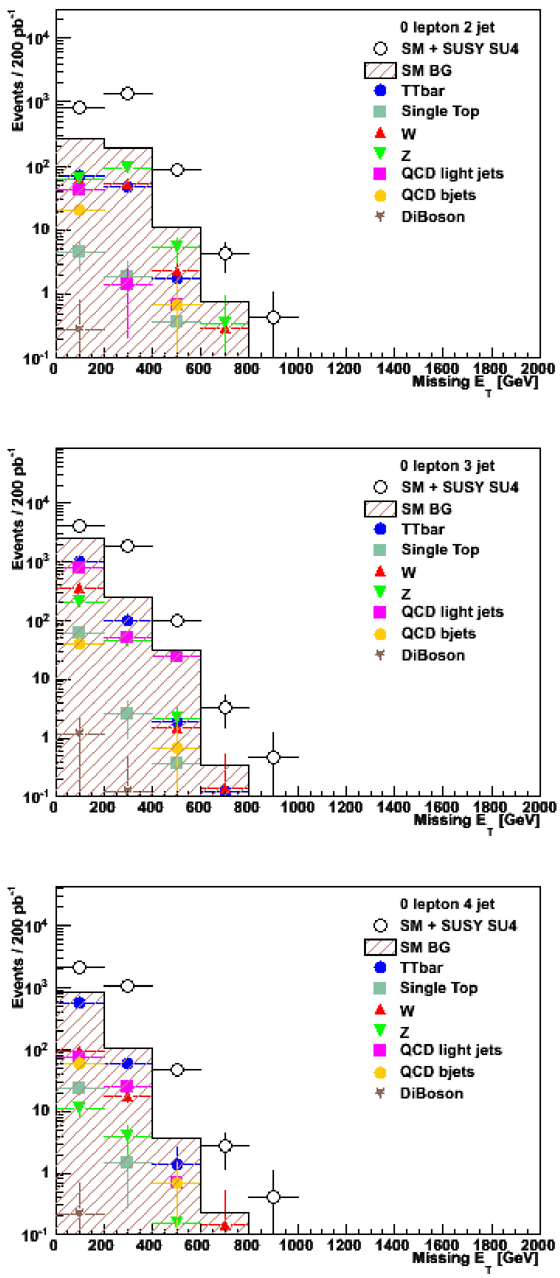

Figure 7: Missing transverse energy for the zero-lepton channel. The plot scheme is the same as in Figure 8.

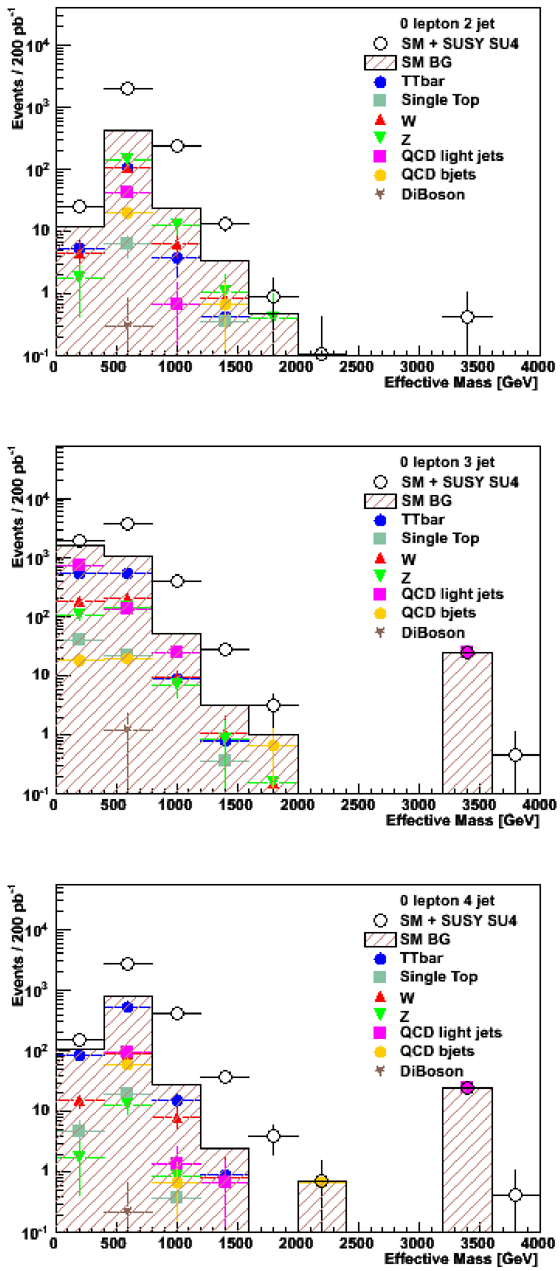

Figure 8: Effective mass for the zero-lepton channel. The coloured markers represent each individual background, and the shaded histogram, their sum. The open circles are the SUSY SU4 signal plus the background. The y-axis is the number of events in a 200 pb^{-1} sample of data.

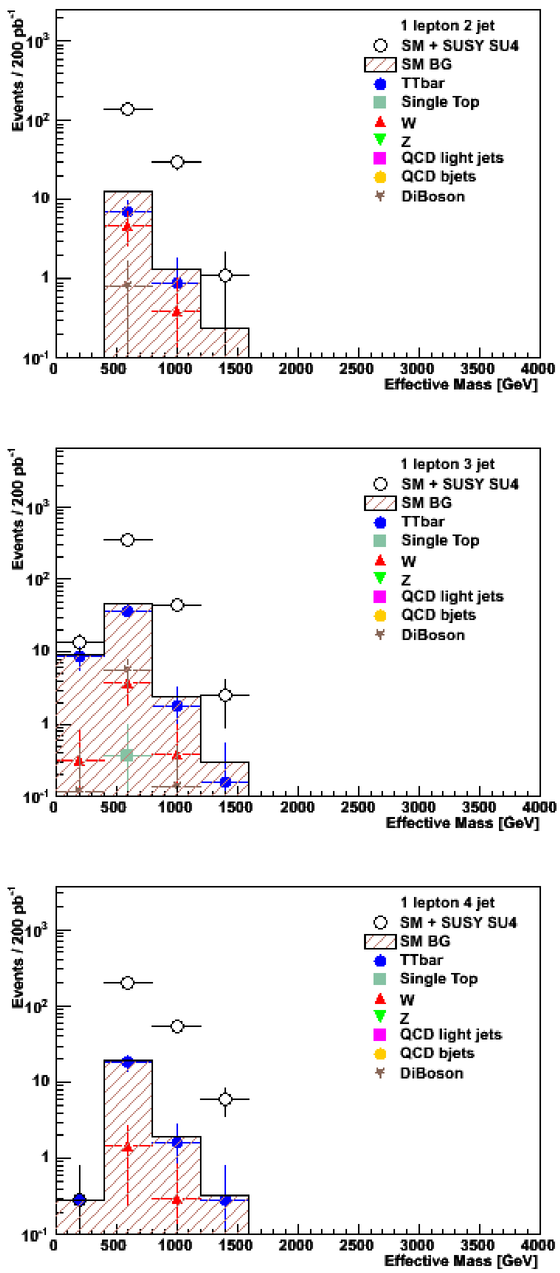

Figure 9: Effective mass for the one-lepton channel. The plot scheme is the same as in Figure 8.

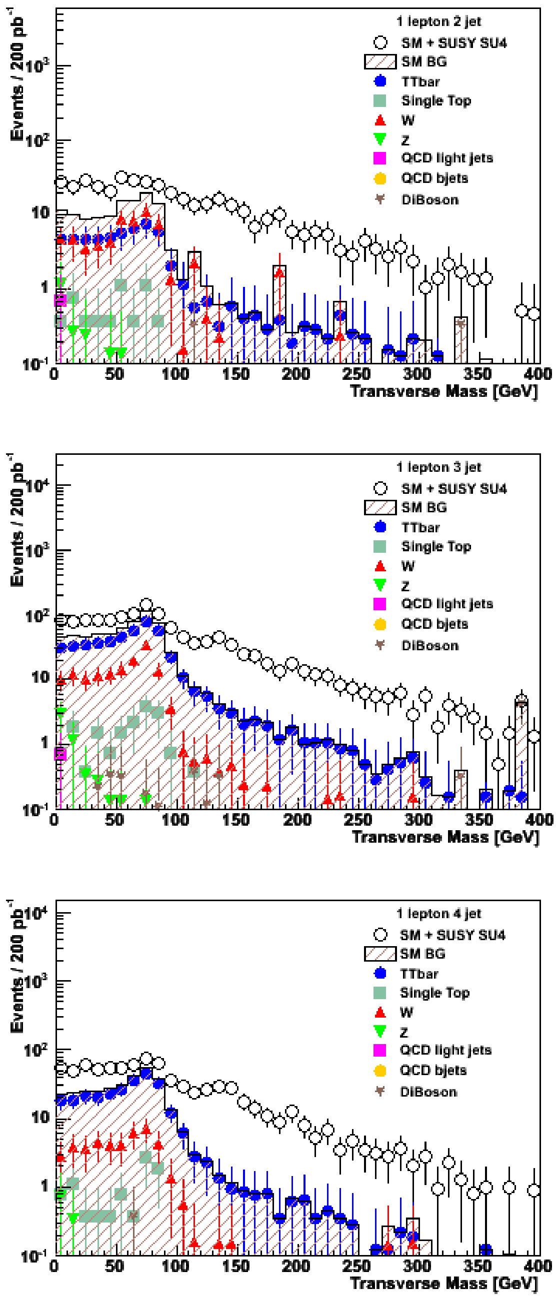

Figure 10: Transverse Mass for the one-lepton channel. The plot scheme is the same as in Figure 8.

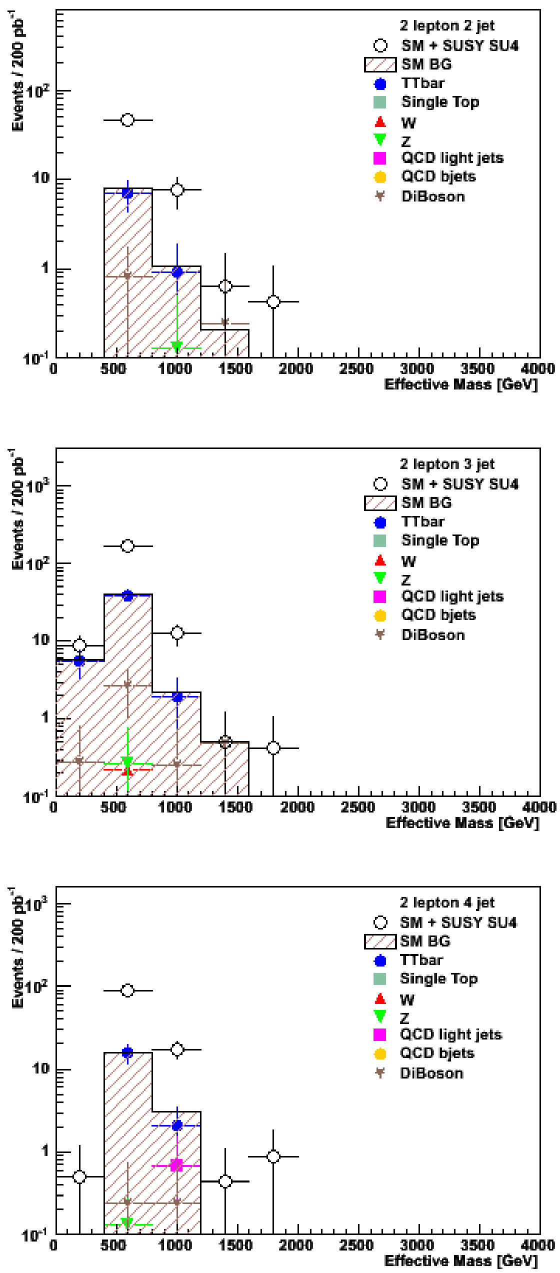

Figure 11: Effective mass for the two-lepton channel. The plot scheme is the same as in Figure 8.

6 Acknowledgements

We would like to thank our supervisor Dr. Richard Teuscher for all of his guidance, as well many colleagues who have helped along the way including Travis Bain, Doug Schouten, Dr. Neil Knecht and Dr. Adam Gibson. We would also like to thank the Institue of Particle Physics and the National Science and Engineering Research Council of Canada for funding this research.

References

[1] S. P. Martin, *A Supersymmetry Primer*, hep-ph/9709356 (1997).

[2] The ATLAS Collaboration, *Supersymmetry Searches*, Expected performance of the ATLAS Experiment - Detector, Trigger and Physics, page 1514-1524, (2009).

[3] The ATLAS Collaboration, *Prospects for Supersymmetry and Universal Extra Dimensions discovery based on inclusive searches at a 10 TeV centre-of-mass energy with the ATLAS detector*, ATLAS-PHYS-PUB-2009-84, (2009).

[4] The ATLAS collaboration, *Prospects for Supersymmetry Discovery based on Inclusive Searches*, Expected performance of the ATLAS Experiment Detector, Trigger and Physics, page 1589-1616, arXiv:0901.0512, (2009).